

Magnetic and magneto-transport properties of double perovskite $\text{Sr}_2\text{FeMoO}_6$ with Co doping

This article has been downloaded from IOPscience. Please scroll down to see the full text article.

2007 J. Phys.: Condens. Matter 19 026215

(<http://iopscience.iop.org/0953-8984/19/2/026215>)

View [the table of contents for this issue](#), or go to the [journal homepage](#) for more

Download details:

IP Address: 129.252.86.83

The article was downloaded on 28/05/2010 at 15:20

Please note that [terms and conditions apply](#).

Magnetic and magneto-transport properties of double perovskite $\text{Sr}_2\text{FeMoO}_6$ with Co doping

Xianjie Wang¹, Yu Sui^{1,2,5}, Jinguang Cheng¹, Zhengnan Qian¹,
Jipeng Miao¹, Zhiguo Liu¹, Ruibin Zhu¹, Wenhui Su^{1,2}, Jinke Tang³ and
C K Ong⁴

¹ Center for Condensed Matter Science and Technology (CCMST), Department of Physics, Harbin Institute of Technology, Harbin 150001, People's Republic of China

² International Centre for Materials Physics, Chinese Academy of Sciences, Shenyang 110016, People's Republic of China

³ Department of Physics, University of New Orleans, New Orleans, LA 70148, USA

⁴ Center for Superconducting and Magnetic Materials and Department of Physics, National University of Singapore, 2 Science Drive 3, 117542, Singapore

E-mail: suiyu@hit.edu.cn

Received 29 September 2006, in final form 22 November 2006

Published 15 December 2006

Online at stacks.iop.org/JPhysCM/19/026215

Abstract

The electrical, magnetic and magnetoresistance properties of polycrystalline $\text{Sr}_2\text{Fe}_{1-x}\text{Co}_x\text{MoO}_6$ compounds with $x = 0.0, 0.05, 0.15$ and 0.25 were investigated. With increasing Co content, both the degree of cationic order and the saturation magnetic moment per formula unit of these compounds increase, while their resistivity decreases monotonically and exhibits an enhanced metallic behaviour for $x \geq 0.15$. The low-field magnetoresistance was greatly enhanced at $x = 0.15$, and the field dependence of magnetoresistance for $x \geq 0.15$ almost saturates above 1.5 T. These results can be well explained by the change of magnetic structure of $\text{Sr}_2\text{FeMoO}_6$ after replacing partial Fe ions by Co ions. The enhanced metallic behaviour and low-field magnetoresistance also suggest a great application potential in spin electronic devices.

1. Introduction

Recently, the magneto-transport property of the half-metallic ferromagnet $\text{Sr}_2\text{FeMoO}_6$ (SFMO) has attracted increasing attention because its large room-temperature magnetoresistance (MR) and high Curie temperature of $T_C \approx 410$ K make it a potential candidate for spintronic device application [1]. SFMO is an ordered double perovskite ($\text{A}_2\text{B}'\text{B}''\text{O}_6$), where the Fe^{3+} and Mo^{5+} ions are spatially distributed alternately in the B-site of the perovskite structure. The antiferromagnetic coupling of Fe^{3+} ($3d^5; t_{2g}^3 e_g^2$) and Mo^{5+} ($4d^1; t_{2g}^1$) ions leads to an expected

⁵ Author to whom any correspondence should be addressed.

saturated moment M_S per formula unit of $4 \mu_B$. However, all the M_S values of bulk SFMO reported so far are smaller than this predicted value due to the presence of naturally grown anti-site defects, where the partial Fe(Mo) ions are misplaced at Mo(Fe) sites in the polycrystalline SFMO compound [1–7].

It is well known that both large low-field MR (LFMR) and high conductivity are necessary for the application of the MR effect. The large LFMR of SFMO, which is believed to be rooted in the spin-dependent scattering at the grain boundary, can be achieved by modulating the grain boundary in SFMO [8–10]. In addition, the LFMR was found to be enhanced by doping at the Fe site [11]. However, single-crystalline $\text{Sr}_2\text{Fe}_{1-x}\text{Co}_x\text{MoO}_6$ (SFCMO) is the only system reported so far in which the conductivity and LFMR were enhanced simultaneously [12–15], suggesting a great application potential in spin electronic devices. But the mechanism for the reduction of resistivity by Co doping has not been settled yet [13]. Moreover, although the double perovskite $\text{Sr}_2\text{CoMoO}_6$ (SCMO) is known as an antiferromagnetic insulator with $T_N = 34$ K, a ferromagnetic behaviour with high Curie temperature ($T_C = 380$ K) and large MR have been achieved in SCMO annealed in a H_2/N_2 atmosphere [16]. Therefore, it is worthwhile investigating the influence of the substitution of Co for Fe ions.

In this paper, we present a detailed study on the electrical and magnetic properties of SFMO doped with Co at the Fe site. We aim to clarify the effect of doping Co ions on the magnetic structure and MR by determining the electronic configuration of Co ions and the magnetic interactions between Fe and Co ions, which will be helpful in the development of magnetoelectronic devices.

2. Experimental details

A series of $\text{Sr}_2\text{Fe}_{1-x}\text{Co}_x\text{MoO}_6$ (SFCMO) ($x = 0.0, 0.05, 0.15, 0.25$) polycrystalline samples was prepared by conventional solid-state reaction. A mixture of high-purity SrCO_3 , Fe_2O_3 , Co_2O_3 and MoO_3 was pressed into pellets and calcined in air at 900°C for 3 h. The pellets were then reground, pressed and reheated with sintering at 1200°C for 1 h in a stream of 1.5% H_2/N_2 . X-ray diffraction (XRD) powder patterns were collected using a Bede D¹ XRD spectrometer with Ni-filtered $\text{Cu K}\alpha$ radiation. The room-temperature XRD patterns were refined by the Rietveld method using the program FullProf [17, 18]. The resistivity was measured using a DC four-probe method and magnetization measurement was carried out using a Quantum Design physical properties measurement system (PPMS).

3. Results and discussion

The XRD patterns of SFCMO polycrystalline samples reveal that all compounds form a good-quality solid solution [19], in which no impurity phase is observed, and that the structure of SFMO does not vary with Co concentration. The XRD pattern of the $x = 0.25$ sample is displayed in figure 1 as an example. Refinements using the tetragonal $I4/mmm$ space group led to the smallest quality-of-fit parameters ($R_{\text{Bragg}} = 3.5$, $S = 1.6$), as found for SFMO [12, 20]. R_p and R_{wp} are 8.2% and 8.8%, respectively. Other XRD patterns were also well refined using the same space group. The degree of cationic disorder, p , which is defined as the fraction of Fe(Mo) ions misplaced at Mo(Fe) sites, can be calculated from the refinement of XRD patterns [19, 21]. As the concentration of Co increases from zero to 25%, p decreases from 15% to 9%, as shown in the inset of figure 1, meaning the improvement of cationic order in SFCMO with doping Co at the Fe site.

Figure 2 shows the isothermal magnetization curve of the sample with $x = 0.25$ at 5 K and in a magnetic field up to 5 T. The magnetization (M) rises rapidly with H and nearly saturates

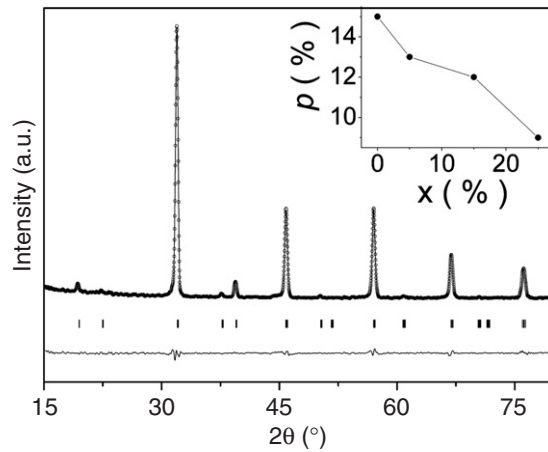


Figure 1. The experimental (open circle) and calculated (solid line) x-ray diffraction patterns for the $x = 0.25$ sample. (R_p and R_{wp} are 8.2% and 8.8%, respectively.) The inset shows the variation of the degree of cationic disorder p with Co content.

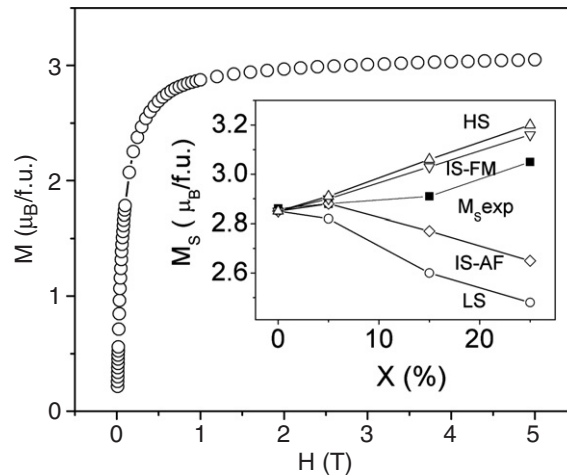


Figure 2. The $M-H$ curves of the sample with $x = 0.25$ at 5 K and up to 5 T. The inset shows the variation of experimental (solid square) and calculated (open symbol) data of M_S with x for SFCMO at 5 K.

at 1 T. Other samples have similar features. The inset of figure 2 shows the variation of the saturation magnetic moment (M_S) per formula unit (f.u.) with doping parameter x at 5 K and 5 T. The value of M_S is only $2.86 \mu_B$ for pure SFMO, which is much lower than its theoretical value of $4 \mu_B$, indicating the existence of many anti-site defects [2–7]. However, it is very interesting that the M_S of SFCMO increases monotonically with increasing Co concentration, as shown in the inset of figure 2, because the magnetic moment of Fe^{3+} ion ($5 \mu_B$) is larger than that of the Co^{3+} ion, even in the case of the high-spin state of Co^{3+} .

The state of the doped Co ions is a key issue for understanding the change of magnetic structure and magneto-transport in SFCMO. In SFCMO, Co may exist as Co^{2+} and/or Co^{3+} ions. If Co^{2+} ions exist, antiferromagnetic insulating SCMO will form [16]. However, the decrease of the resistivity of SFCMO with Co content, which will be shown later (figure 3),

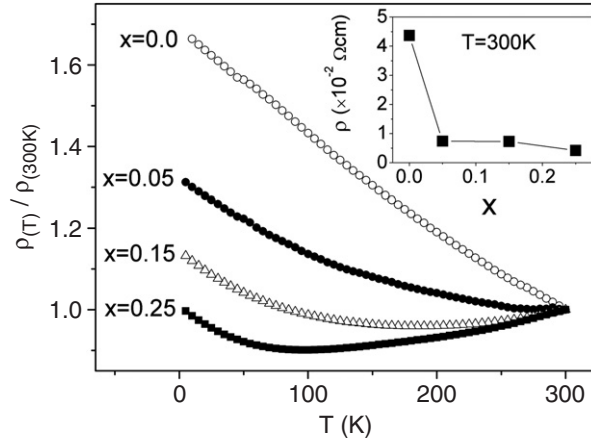


Figure 3. Temperature dependence of the zero-field resistivity of samples with different doping concentration x .

suggests that there is no SCMO forming in our samples or that the amount of SCMO is so small that it has no detectable influence on the magnetic and magneto-transport properties of the samples. Moritomo *et al* also suggested that Co exists as Co^{3+} ions in single-crystal SFCMO up to 40% doping concentration [13]. Thus, it can be concluded that only Co^{3+} ions exist in our SFCMO samples. There are three possible spin configurations of Co^{3+} ion at the octahedral site, depending on the competition between the crystal-field splitting and the intra-atomic Hund exchange-field splitting; i.e. low-spin state (LS, $t_{2g}^6 e_g^0$, $S = 0$), intermediate-spin state (IS, $t_{2g}^5 e_g^1$, $S = 1$), and high-spin state (HS, $t_{2g}^4 e_g^2$, $S = 2$). In the first case, the LS Co^{3+} ion has no contribution to M_S , and then the magnetic moment of SFCMO can be described as [3, 4]

$$M_S = [4(1 - 2p) - x(4 - 9p)]\mu_B \quad (1)$$

which is similar to that of doping nonmagnetic Al ions in SFMO [11]. Here, p is the degree of cationic disorder. Obviously, M_S decreases as x increases and its calculated value is much lower than the experimental data, as shown in the inset of figure 2 (open circle). In the latter two cases, antiferromagnetic Fe–O–Fe pairs would change into ferromagnetic Co–O–Fe pairs when some Fe ions in the anti-site regions were substituted by Co, as has been reported in the ferromagnetic $\text{Sr}_2\text{FeCoO}_6$ [22]. The contribution from the ferromagnetic coupling of Co–O–Fe pairs in the anti-site regions would lead to the enhancement of M_S . For the case of IS Co^{3+} ($2\mu_B$), if Co^{3+} couples with Mo^{5+} antiferromagnetically in the normal region, the magnetic moment of SFCMO will be given as

$$M_S = [4(1 - 2p) - x(3 - 10p)]\mu_B \quad (2)$$

where $x(3 - 10p)$ is also from the doped Co ion. The value of M_S calculated by equation (2) is also lower than the experimental data and decreases as x increases, as shown in the inset of figure 2 (open squares). However, it should be noted that there is one empty e_g orbit in each Co^{3+} ion with IS, and thus the itinerant d electron of Mo^{5+} ($4d^1:t_{2g}^1$) may occupy this orbit. Therefore, a ferromagnetic coupling $\text{Co}^{3+}\text{--O--Mo}^{5+}$ pair could be expected in SFCMO, which can lead to the increase of M_S . Based on the above analysis, the magnetic moment of SFCMO can be changed into

$$M_S = [4(1 - 2p) - x(1 - 8p)]\mu_B \quad (3)$$

where $x(1 - 8p)$ is also from the contribution of doped Co. In the third case (HS Co^{3+} , $4\mu_{\text{B}}$), the Co^{3+} ions can only couple with Mo^{5+} ions antiferromagnetically. Taking account of the contribution of ferromagnetic coupling of Co–O–Fe pairs in anti-site regions, the magnetic moment of SFCMO can be described as

$$M_{\text{S}} = [4(1 - 2p) - x(1 - 10p)]\mu_{\text{B}}. \quad (4)$$

It is clear from the inset of figure 2 (open down-triangle and up-triangle) that the values of M_{S} calculated from equations (3) and (4) are very similar, and the equations satisfactorily explain reproducing the evolution of M_{S} of SFCMO. The difference between the calculated results and the measurement value may be caused by the fact that we did not consider the effect of antiferromagnetic coupled Co–O–Co pairs in these two equations; these pairs may form in the anti-site regions and lead to the reduction of M_{S} .

Although the HS and IS Co^{3+} with spins antiparallel and parallel to the neighbour Mo^{5+} spins, respectively, can all be anticipated from the analysis of the saturation magnetic moment, the IS configuration of Co^{3+} can be ruled out from the variation of resistivity with Co concentration. As shown in figure 3, the semiconductive behaviour observed in SFCMO samples with $x < 0.15$, rather than the half-metallic character of SFMO single crystal, may arise from the scattering of electrons at grain boundaries or anti-site defects [19]. However, the resistivity of SFCMO in the whole temperature range decreases monotonically with increasing x , and the SFCMO samples with $x \geq 0.15$ show a metallic-like conducting behaviour at high temperature. Such an enhancement of electrical conduction in Co-doped SFMO has been observed in single-crystal samples, but its mechanism has not been clarified [13]. Although the contribution of the grain boundary to the measured resistivity cannot be avoided for polycrystalline samples, the monotonic reduction of resistivity of SFCMO polycrystalline samples should be an intrinsic feature, just like that of single crystals, because all these samples were prepared using the same process. Based on the above analysis of M_{S} , if the Co^{3+} ions exist as the IS configuration, the itinerant electron of Mo^{5+} will be confused by the confliction between the antiparallel arrangement with the neighbour Fe^{3+} and then parallel arrangement with the IS Co^{3+} . This will no doubt cause an increase rather than a decrease of resistivity. Instead, the HS Co^{3+} ions can maintain the original antiferromagnetic coupling between the spin of itinerant Mo^{5+} electrons and the $\text{Fe}^{3+}/\text{Co}^{3+}$ moments. Therefore, the doped Co ions should be HS trivalent and the increase of M_{S} originates from the replacement of antiferromagnetic Fe–O–Fe by the ferromagnetic Fe–O–Co pairs in the anti-site region. Such ferromagnetic Fe–O–Co pairs will not only reduce the spin-dependent scattering at the original antiferromagnetic Fe–O–Fe, but also lead to the formation of the metallic Fe–O–Co paths as discovered in $\text{Sr}_2\text{FeCoO}_6$ [22]. Moreover, in contrast to the empty spin-down Fe t_{2g} bands, the HS Co^{3+} leaves one electron in the spin-down t_{2g} bands, which might overlap and broaden the itinerant Fe/Mo t_{2g} bands and thus reduce the resistivity. With increasing Co content, the resistivity of SFCMO will decrease gradually, and a semiconductor–metal transition occurs at the threshold of $x = 0.15$. Furthermore, the monotonic decrease of resistivity with the increase of Co content means that the contribution of the grain boundaries to the total resistivity increases gradually. So the LFMR of SFMO, which is usually considered to arise from the spin-dependent scattering at grain boundaries, can be enhanced by doping Co.

The dependence of MR on doping concentration at 5 K for SFCMO samples in a magnetic field up to 5 T is shown in figure 4. The MR is defined as

$$\text{MR}(T, H) = 100\% \times [\rho(T, 0) - \rho(T, H)]/\rho(T, 0) \quad (5)$$

where $\rho(T, 0)$ and $\rho(T, H)$ are the resistivity of the sample at zero field and external field H , respectively. The LFMR of SFCMO was enhanced remarkably for $x = 0.15$. The role of Co in the doped SFMO sample is to strengthen the ferromagnetic coupling and to enhance the

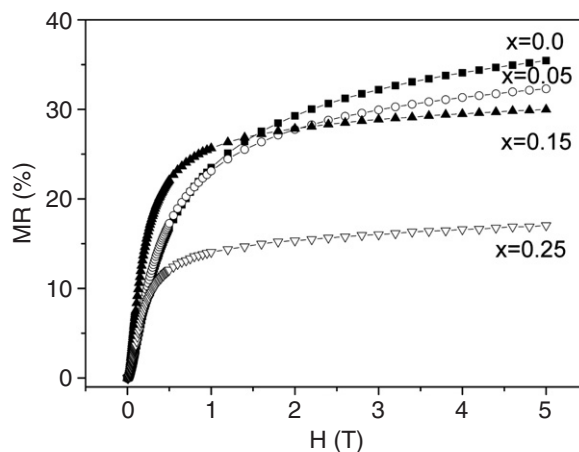


Figure 4. The magnetic field dependence of MR of samples with different doping concentration x at 5 K.

conduction. On the one hand, the improvement of cationic order in SFCMO may enhance the LFMR [7, 19]. On the other hand, the enhanced metallic conduction means that the contribution of spin-dependent scattering at the grain boundaries to the total resistivity increases gradually. Thus the LFMR increases with increasing Co content and will be enhanced remarkably near the optimum value ($x = 0.15$), which is the threshold for the semiconductor–metal transition. When the doping parameter x is larger than the optimum value, the sample become metallic and the LFMR is suppressed.

It is worth mentioning that the MR curves show weak magnetic field dependence under high field with increasing x . As displayed in figure 4, the MR of the samples for $x \geq 0.15$ almost saturates above 1.5 T, and the saturation value is lower than the maximum theoretical value for half-metals (50%) predicted by the direct tunnelling model [23]. The saturated MR curve of double perovskite $\text{Ba}_{1.6}\text{Sr}_{0.4}\text{FeMoO}_6$ was observed above 40 T by Serrate *et al* [23], but there are few reports of the saturated MR curve of SFMO below 5 T so far. The high-field MR is intrinsic MR as observed in SFMO single crystal, which mainly originates from the progressive alignment of antiferromagnetic Fe–O–Fe with increasing magnetic field [21]. The saturated MR curves of $x \geq 0.15$ above 1.5 T can be explained by a decrease or the disappearance of antiferromagnetic Fe–O–Fe pairs after Co doping. Based on the above structural analysis, the anti-site defects were suppressed by the improvement of cationic order. Furthermore, the formation of ferromagnetic Fe–O–Co pairs at the abnormal Fe sites also destroy the antiferromagnetic Fe–O–Fe. Thus, the magnetic field for aligning the antiferromagnetic Fe–O–Fe will decrease and the MR curves will saturate easily at a relative low field.

4. Conclusion

In summary, based on the analysis of M_S and resistivity, we suggest that the doped Co ions may be HS trivalent in SFCMO, and that the role of doped Co is to broaden the minority-spin Mo/Fe t_{2g} band and change some antiferromagnetic insulating Fe–O–Fe pairs in anti-site regions into ferromagnetic metallic Fe–O–Co pairs. Therefore, the M_S of SFCMO compounds increases while their resistivity decreases monotonically with increasing Co content. At $x = 0.15$, which

is located near the insulator–metal boundary, the SFCMO compound gives the largest LFMR, and shows a saturated MR(H) curve due to the disappearance of antiferromagnetic Fe–O–Fe pairs in anti-site regions by Co doping.

Acknowledgments

This work was supported by the National Natural Science Foundation of China (Grant Nos 10304004 and 50672019).

References

- [1] Kobayashi K I, Kimura T, Sawada H, Terakura K and Tokura Y 1998 *Nature* **395** 677
- [2] Sakuma H, Taniyama T, Kitamoto Y and Yamazaki Y 2003 *J. Appl. Phys.* **93** 2816
- [3] Ogale A S, Ogale S B, Ramesh R and Venkatesan T 1999 *Appl. Phys. Lett.* **75** 537
- [4] Balcells L I, Navarro J, Bibes M, Roig A, Martíne B and Fontcuberta J 2001 *Appl. Phys. Lett.* **78** 781
- [5] Navarro J, Balcells L I, Sandiumenge F, Bibes M, Roig A, Martínez B and Fontcuberta J 2001 *J. Phys.: Condens. Matter* **13** 8481
- [6] Lindén J, Karppinen M, Shimada T, Yasukawa Y and Yamauchi H 2003 *Phys. Rev. B* **68** 174415
- [7] García-Hernández M, Martínez J L, Martínez-Lope M J, Casais M T and Alonso J A 2001 *Phys. Rev. Lett.* **86** 2443
- [8] Yin H Q, Zhou J-S, Zhou J-P, Dass R, McDevitt J T and Goodenough J B 1999 *Appl. Phys. Lett.* **75** 2812
- [9] Yuan C L, Wang S G, Song W H, Yu T, Dai J M, Ye S L and Sun Y P 1999 *Appl. Phys. Lett.* **75** 3853
- [10] Niebieskikwiat D, Caneiro A, Sánchez R D and Fontcuberta J 2001 *Phys. Rev. B* **64** 180406
- [11] Sui Y, Wang X J, Cheng J G, Liu Z G, Miao J P, Huang X Q, Lu Z, Qian Z N, Su W H, Tang J K and Ong C K 2005 *J. Appl. Phys.* **98** 064505
- [12] Feng X M, Rao G H, Liu G Y, Yang H F, Liu W F, Ouyang Z W, Yang L T, Liu Z X, Yu R C, Jin C Q and Liang J K 2002 *J. Phys.: Condens. Matter* **14** 12503
- [13] Moritomo Y, Kusuya H, Akimoto T and Machida A 2000 *Japan. J. Appl. Phys.* **39** L360
- [14] Yuan C L, Zhu Y and Ong P P 2002 *J. Appl. Phys.* **91** 4421
- [15] Chen L, Yuan C L, Xue J M and Wang J 2005 *J. Phys. D: Appl. Phys.* **38** 4003
- [16] Viola C, Martínez-Lope M J, Alonao J A, Velasco P, Martínez J L, Pedregosa J C, Carbonio R E and Fernández-Díaz M T 2002 *Chem. Mater.* **14** 812
- [17] Rietveld H M 1967 *Acta Crystallogr.* **22** 151
- [18] Rodríguez-Carvajal J 1993 *Physica B* **192** 55
- [19] Sarma D D, Sampathkumaran E V, Ray S, Nagarajan R, Majumdar S, Kumar A, Nalini G and Guru Row T N 2000 *Solid State Commun.* **114** 465
- [20] Rubi D, Frontera C, Nogués J and Fontcuberta J 2004 *J. Phys.: Condens. Matter* **16** 3173
- [21] Tomioka Y, Okuda T, Okimoto Y, Kumai R, Kobayashi K I and Tokura Y 2000 *Phys. Rev. B* **61** 422
- [22] Abbate M, Zampieri G, Okamoto J, Fujimori A, Kawasaki S and Takano M 2002 *Phys. Rev. B* **65** 165120
- [23] Serrate D, De Teresa J M, Algarabel P A, Ibarra M R and Galibert J 2005 *Phys. Rev. B* **71** 104409